Neurobiology of Disease 76 (2015) 77–86

Contents lists available at ScienceDirect

Neurobiology of Disease

journal homepage: www.elsevier.com/locate/ynbdi

Administration of CoQ_{10} analogue ameliorates dysfunction of the mitochondrial respiratory chain in a mouse model of Angelman syndrome

Katrina J. Llewellyn [a,*], Angèle Nalbandian [a], Arianna Gomez [a], Don Wei [b], Naomi Walker [a], Virginia E. Kimonis [a,**]

[a] Department of Pediatrics, Division of Genetics and Genomics, 2501 Hewitt Hall, University of California-Irvine, Irvine, CA 92697, USA
[b] Department of Anatomy & Neurobiology, Gillespie Hall, University of California-Irvine, Irvine, CA 92697, USA

ARTICLE INFO

Article history:
Received 6 August 2014
Revised 23 December 2014
Accepted 25 January 2015
Available online 12 February 2015

Keywords:
Neurodegenerative disorder
Angelman syndrome
Mitochondrial respiratory chain
Coenzyme Q_{10} analogue
Idebenone
Cytochrome oxidase subunit IV
Glutathione disulfide

ABSTRACT

Genetic defects in the *UBE3A* gene, which encodes for the imprinted E6-AP ubiquitin E3 ligase (UBE3A), is responsible for the occurrence of Angelman syndrome (AS), a neurodegenerative disorder which arises in 1 out of every 12,000–20,000 births. Classical symptoms of AS include delayed development, impaired speech, and epileptic seizures with characteristic electroencephalography (EEG) readings. We have previously reported impaired mitochondrial structure and reduced complex III in the hippocampus and cerebellum in the *Ube3a*$^{m-/p+}$ mice. CoQ_{10} supplementation restores the electron flow to the mitochondrial respiratory chain (MRC) to ultimately increase mitochondrial antioxidant capacity. A number of recent studies with CoQ_{10} analogues seem promising in providing therapeutic benefit to patients with a variety of disorders. CoQ_{10} therapy has been reported to be safe and relatively well-tolerated at doses as high as 3000 mg/day in patients with disorders of CoQ_{10} biosynthesis and MRC disorders. Herein, we report administration of idebenone, a potent CoQ_{10} analogue, to the *Ube3a*$^{m-/p+}$ mouse model corrects motor coordination and anxiety levels, and also improves the expression of complexes III and IV in hippocampus CA1 and CA2 neurons and cerebellum in these *Ube3a*$^{m-/p+}$ mice. However, treatment with idebenone illustrated no beneficial effects in the reduction of oxidative stress. To our knowledge, this is the first study to suggest an improvement in mitochondrial respiratory chain dysfunction via bioenergetics modulation with a CoQ_{10} analogue. These findings may further elucidate possible cellular and molecular mechanism(s) and ultimately a clinical therapeutic approach/benefit for patients with Angelman syndrome.

Introduction

Genetic defects in the *UBE3A* gene which encodes for E6-AP ubiquitin-protein ligase E3A (UBE3A), also known as E6-AP ubiquitin protein ligase, are responsible for the occurrence of Angelman syndrome (AS), a neurodegenerative disorder that arises in 1 in every 12,000–20,000 births (Hasegawa et al., 2012; Kishino et al., 1997; Knoll et al., 1989). Symptoms of AS include delayed development, severely impaired speech, ataxia, microcephaly and epileptic seizures with characteristic EEG readings (Bailus & Segal, 2014; Bird, 2014). Maternal deletions or paternal uniparental disomy of chromosomal 15q11-13 region accounts for 70% and 7%, respectively of Angelman syndrome. An additional 11% is due to point mutations or deletions of the *UBE3A* gene and 3% is accounted for by imprinting center defects (Kishino et al., 1997; Knoll et al., 1989; Jiang et al., 1998a; Jiang et al., 1998b; Nicholls et al., 1998).

Ubiquitin E3 ligase is important in several cellular functions, including protein degradation, protein transport, endocytosis and protein–protein interactions. Jiang et al. (1998a) generated and characterized the *Ube3a*$^{m-/p+}$ as an Angelman mouse model, having a deletion of the maternal *UBE3A* copy (Jiang et al., 1998a; Jiang et al., 1998b). Due to paternal imprinting, the *UBE3A* gene is silenced in certain brain regions, including the hippocampus and cerebellum, resulting in a lack of the UBE3A protein expression (Kishino et al., 1997; Jiang et al., 1998a). These mice exhibit pathology characteristic of Angelman syndrome, including motor coordination issues (ataxia), microcephaly, and epileptic-like seizures. These mice also display defects in the hippocampal long-term potentiation and cerebellar motor function (Huang et al., 2013; Gabriel et al., 1999). Our previous studies have demonstrated that hippocampal mitochondria of *Ube3a*$^{m-/p+}$ mice are small and dense with disorganized cristae. These mice depict a reduction of complex III activity in the hippocampal region of the brain (Su et al., 2011). Several diseases with similar symptoms to AS, such as Rett syndrome

* Corresponding author. Tel.: +1 949824 7964.
** Corresponding author. Tel.: +1 714 456 5791, +1 714 456 2942 (direct); fax: +1 714 456 5330, +1 714 506 2063 (pager).
E-mail addresses: kllewell@uci.edu (K.J. Llewellyn), vkimonis@uci.edu (V.E. Kimonis).
Available online on ScienceDirect (www.sciencedirect.com).

http://dx.doi.org/10.1016/j.nbd.2015.01.005
0969-9961/

have mitochondrial abnormalities (Condie et al., 2010; Gold et al., 2014). Our initial results that were suggestive of mitochondrial dysfunction in human AS led to this current investigation.

Idebenone is a CoQ_{10} analogue, the predominant form of ubiquinone in humans. To date, the only agents which have shown some therapeutic potential have been CoQ_{10} and its synthetic analogues. Idebenone is currently being used for the treatment of mitochondrial respiratory chain (MRC) disorders, which have been difficult to treat. We report that administration of idebenone, to the *Ube3a*$^{m-/p+}$ mouse system corrects motor coordination and anxiety levels, but does not affect brain size, sociability or memory by novel object recognition (NOR) assay. We report that CoQ_{10} treatment also improves the expression of complexes III and IV in the neurons of hippocampus CA1, CA2, and CA3 regions of the *Ube3a*$^{m-/p+}$ mice. In addition, we report that oxidative stress measured by levels of glutathione disulfide (GSSG:GSH) and 4-HNE were increased in the cerebellum and hippocampus of *Ube3a*$^{m-/p+}$ mice, when compared to WT controls. To our knowledge, this is the first study to suggest an improvement in the dysfunction of the mitochondrial respiratory chain with a CoQ_{10} analogue, further elucidating a possible cellular/molecular mechanism(s) and ultimately potential therapeutic benefits for patients with Angelman syndrome.

Materials and methods

Ethical statement

All experiments were done with the approval of the Institutional Animal Care and Use Committee (IACUC) of the University of California, Irvine (UCI) (IACUC Protocol #2007-2716-2), and in accordance with the guidelines established by the National Institutes of Health (NIH). Animals were housed in the vivarium and maintained under constant temperature (22 °C) and humidity with a controlled 12:12-hour light–dark cycle. Mice were provided standard rodent chow (Harlan Teklad Rodent Diet, Madison, WI) and water ad libitum. Mouse genotyping was performed at Transnetyx Inc., (ordova, TN).

Idebenone administration

Three-week old WT and *Ube3a*$^{m-/p+}$ mice on a C56BL/6 J background were randomly sorted into either treatment or control groups (n = 8–10 per group). Idebenone at 200 mg/kg body weight dissolved in corn oil was administered to the WT and *Ube3a*$^{m-/p+}$ groups by oral gavage, whereas the control groups received corn oil (vehicle), three times a week for three months. No adverse effects were noted with either treatment. Body and brain weights from the wild type and *Ube3a*$^{m-/p+}$ mice were recorded.

Behavioral studies

Rotarod performance test

To assess performance measurements, treated and untreated WT and *Ube3a*$^{m-/p+}$ mice were placed on the Rotarod apparatus, which was set to accelerate from 4 to 40 rpm in 5 min. Mice performed three trials with 45-min to 60-min inter-trial intervals on each of two consecutive days. Rotarod measurements were taken before and after idebenone administration.

Marble burying assay

Treated and untreated WT and *Ube3a*$^{m-/p+}$ mice were analyzed with the marble burying assay. Briefly, a cage was filled 5–10 cm deep with bedding spread evenly where twelve black glass marbles, evenly spaced, were placed on the surface of the bedding in four rows of three. Idebenone treated or untreated wild type or *Ube3a*$^{m-/p+}$ mice were placed separately in the cage and left undisturbed for 20 min. The number of marbles buried to 2/3 their depth was then counted and analyzed as previously described (Angoa-Perez et al., 2013).

Social three-chamber assay

The sociability assay was performed as previously described (Kaidanovich-Beilin et al., 2011; Silverman et al., 2010) to evaluate the sociability of treated and untreated WT and *Ube3a*$^{m-/p+}$ mice. Briefly, a rectangular three-chambered box apparatus was used (divided by clear plexiglass walls) with rectangular openings allowing access into each chamber. While one side contained an empty container, the other side of the container housed a mouse. The container had small bars to allow for social interaction. WT or *Ube3a*$^{m-/p+}$ mice treated/untreated with idebenone were first placed in the middle chamber and allowed to acclimatize for 10 min. Once the mouse was acclimatized, barriers separating the two side chambers were removed. The test mouse was left for 10 min to habituate to side chambers with no mouse present (empty apparatus). Finally, the mouse was given 10 min to interact and explore the three chambers when the mouse was present. The "social index" was measured as (chamber time in social chamber − chamber time in object chamber) / (total time in side chambers).

Novel object recognition (NOR) test

In order to assess memory recognition in the treated and untreated WT and *Ube3a*$^{m-/p+}$ mice, we performed novel object recognition (NOR) tests. Briefly, two novelty objects were placed into a sterile cage and fixed in place. Treated and untreated WT and *Ube3a*$^{m-/p+}$ mice were placed alone in the cage. The mouse was left for 15 min to explore and acclimate to the new environment before being moved back to its original cage. This was repeated for all mice twice on day 1 and day 2. On day 3, the acclimation step was repeated in the morning. In the afternoon (at least a 3 hour gap), one of the novel objects was replaced with a new object. Mice were then placed in the cage for 5 min. Mice interactions with the novel objects were recorded. Analysis of assay: Exploration was scored when the mouse touched an object with its forepaws, snout, licked, or sniffed the object from a distance of no more than 1.5 cm. The novelty index (NI) was calculated as NI = (Tn − Tr) / (Tn + Tr) (Silvers et al., 2007). 'Tn' represented the time exploring a novel object and 'Tr' the duration of a familiar object exploration.

Seizure activity and electroencephalogram (EEG) testing

Seizure activity in WT and *Ube3a*$^{m-/p+}$ mice (idebenone-treated and untreated) was monitored. Briefly, seizures were induced by scratching with a pair of long blunt forceps over the cage grid for 45 s and mice were visually monitored. All mice tested were 4–5 months of age. Inducible seizures (typically lasting 10–20 s) were noted when mice responded by increased activity including running and leaping followed by rigid extension of limbs and body (tonic and clonic seizures), as previously described (Jiang et al., 1998b).

In order to examine the characteristic brain activity in the treated and untreated WT and *Ube3a*$^{m-/p+}$ mice, we performed EEG analysis as previously described (Cattanach et al., 1992). Bipolar depth electrodes (PlasticsOne, Roanoke, VA) and optical fibers (0.37 NA, Low OH, 200 μm diameter, ThorLabs, Newton, NJ) terminated in 1.25 mm ceramic ferrules (Kientec Systems, Inc., Stuart, FL) were implanted ipsilaterally (posterior 2.5 mm, left 1.75 mm, ventral 1.25 mm with respect to bregma) and in some cases, also contralaterally at the same posteroventral position into the hippocampus, targeting the dorsal stratum oriens of the CA1 so that emitted light would illuminate the hippocampal formation. Optical fibers and electrodes were fixed to the skull using screws and dental cement (Teets Cold Curing, Sylmar, CA) and the animals were allowed to recover for several days before beginning the 24 hour video and EEG monitoring for seizures and subsequent closed-loop seizure detection and light delivery. EEG activity was monitored by data acquisition system via a lightweight, flexible, shielded, grounded multi-wire cable to ensure optimal recording conditions.

Biochemical assays

Histological staining (H&E) and immunohistochemistry (IHC)

Brain samples from WT and *Ube3a*$^{m-/p+}$ mice (idebenone-treated and untreated) were harvested. After the weight of the brain was recorded, it was hardened in frozen PBS and then the cerebellum and frontal cortex were cut, leaving the hippocampus intact. The hippocampus region was then frozen in isopentane pre-chilled at −40 °C in dry ice. Samples were stored at −80 °C before sectioning at 5–10 μm thickness. Hematoxylin and eosin stains were performed as previously described (Badadani et al., 2010). For immunohistochemical analyses, sections were stained with anti-glial fibrillary acidic protein (GFAP) and complexes III- and IV-specific antibodies (Abcam, Cambridge, MA). Subsequently, sections were washed with PBS and incubated with fluorescein-conjugated secondary antibodies (Sigma-Aldrich, St. Louis, MO) for 1 h at room temperature and mounted with DAPI-containing mounting media (Vector Laboratories, Inc., Burlingame, CA). The CA1, CA2 and CA3 hippocampal regions from WT and *Ube3a*$^{m-/p+}$ mice were analyzed by fluorescence microscopy.

Mitochondrial extractions

Hippocampus and cerebellum samples from WT and *Ube3a*$^{m-/p+}$ mice (idebenone-treated and untreated) were minced in homogenization medium and then homogenized with 2–3 strokes with a Teflon dounce homogenizer. Samples were centrifuged at 800 ×*g* for 10 min at 4 °C. The supernatant was then decanted through two layers of cheesecloth to a separate tube. The final pellet was resuspended in 100 μl MSHE (210 mM mannitol, 70 mM sucrose, 5 mM HEPES, 1 mM EGTA) + BSA (0.5% bovine serum albumin). Samples were stored at -80 °C for future use.

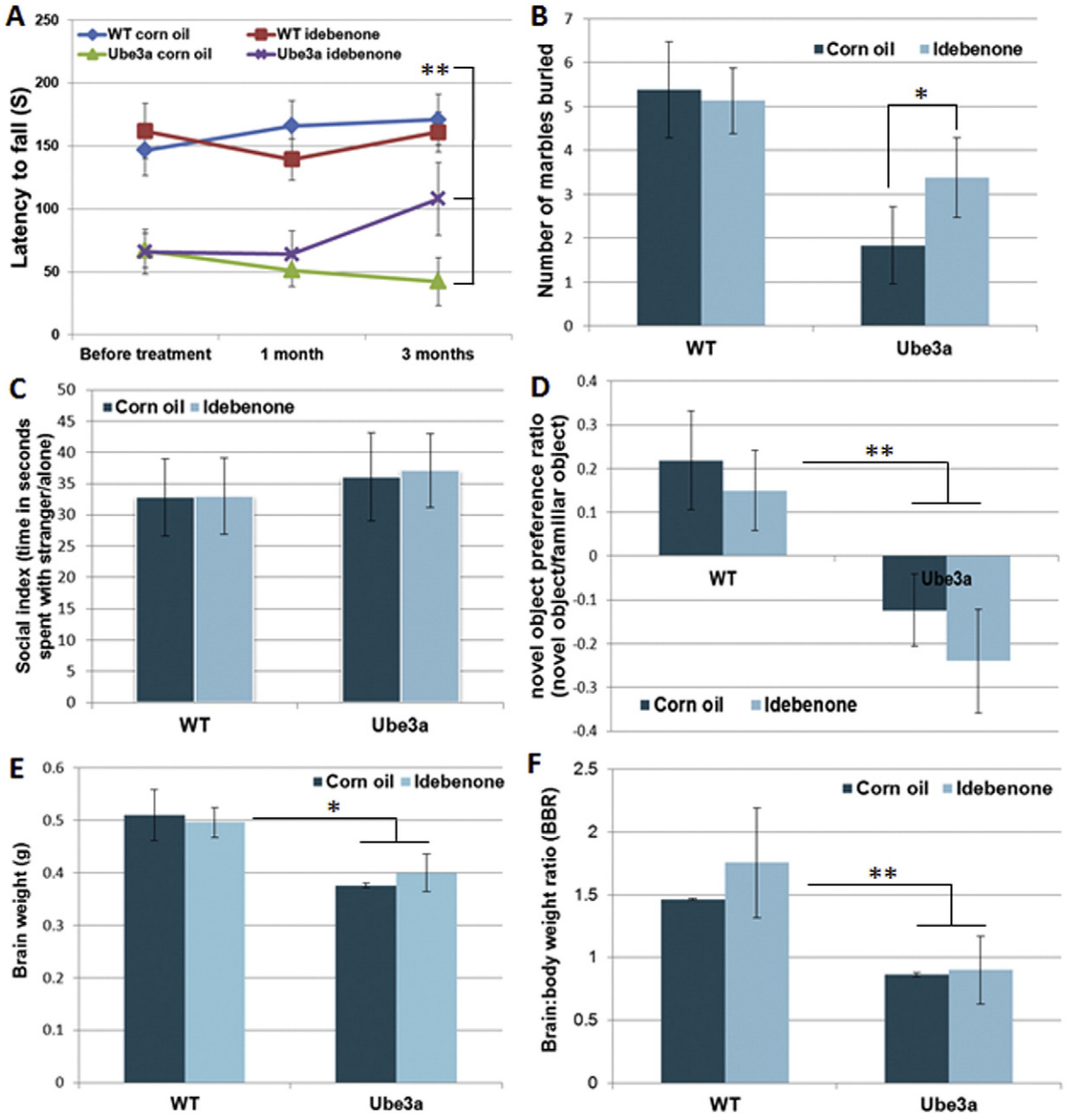

Fig. 1. Rotarod and marble burying assay in *Ube3a*$^{m-/p+}$ mice after idebenone administration. A) Rotarod analysis of WT and *Ube3a*$^{m-/p+}$ mice treated with either corn oil or idebenone 200 mg/kg body weight. B) Marble burying, C) sociability index and D) novel object recognition (NOR) test assays performed on WT and *Ube3a*$^{m-/p+}$ mice treated with either corn oil or idebenone (200 mg/kg body weight) for 3 months. E) Brain weights or F) Brain:body weight ratios of WT and *Ube3a*$^{m-/p+}$ mice treated with either corn oil or idebenone 200 mg/kg body weight for 3 months. Mice were analyzed per treatment group (n = 8–9). Statistical significance is denoted by *P ≤ 0.005 and **P ≤ 0.001.

Protein extraction and quantification

Proteins were extracted from hippocampus and cerebellum mitochondria samples from WT and *Ube3a*$^{m-/p+}$ mice (idebenone-treated and untreated) with RIPA buffer. Protein concentrations were determined using the Nanodrop according to the manufacturer's protocols. Equal amounts of proteins were separated on Bis-Tris 4–12% NuPAGE gels (Invitrogen Life Technologies Inc., Carlsbad, CA), and run on a mini Novex cell for 35 min at 200 V. Primary antibodies against complexes I–IV, 4-HNE, and GFAP from the hippocampal and cerebellar mitochondria were analyzed. All antibodies were purchased from Abcam (Cambridge, MA). Membranes were washed in TBST (0.5%) and probed with anti-mouse or anti-rabbit secondary antibodies for 1 h at room temperature. Membranes were then washed and bands were detected using the Immun-Star™ Western C™ Chemiluminescence kit (Bio-Rad Laboratories, Hercules, CA) as described previously (Nalbandian et al., 2013; Nalbandian et al., 2012). Equal protein loading was confirmed by porin (Abcam) staining.

Complexes I, II, and III activity assays

The enzyme activities of complexes I, II, and III from idebenone-treated and untreated WT and *Ube3a*$^{m-/p+}$ mice were assessed. Briefly, The MitoTox™ OXPHOS Complex III Activity Kit (Abcam, Cambridge, MA) was used to assess complex III activity assays according to manufacturer's instructions. Briefly, 500 μl of complex III activity solution was added to eight 1.5 ml tubes. 100 μl from each tube was transferred into rows A and H as controls. Whole mitochondria extract of hippocampus and cerebellum samples from WT and *Ube3a*$^{m-/p+}$ mice (idebenone-treated and untreated). Controls were added to the eight different 1.5 ml tubes to start the complex III reaction. Samples were mixed and 100 μl of each sample was added to the three corresponding wells in the 96-well plate and analyzed by the microreader machine (Bio-Rad Laboratories, Irvine, CA). The kinetic protocol measured readings at 550 nm every 20 s for 30 min. The V_{max} was then calculated. For complexes I and II, the Complex I Enzyme Activity Microplate Assay Kit (ab109721, Abcam) and Complex II Enzyme Activity Microplate Assay Kit (ab109908, Abcam) were used to examine the enzyme activities in the idebenone-treated and untreated WT and *Ube3a*$^{m-/p+}$ mice as per manufacturer's instructions (Abcam, Cambridge, MA).

Glutathione (GSH) enzyme assay

Glutathione (GSH) was measured of hippocampus and cerebellum samples from WT and *Ube3a*$^{m-/p+}$ mice (idebenone-treated and untreated) using the SensoLyte® Total GSH Assay Kit *Colorimetric* according to manufacturer's instructions (AnaSpec, Fremont, CA). Briefly, we prepared the hippocampus and cerebellum samples from WT and *Ube3a*$^{m-/p+}$ mice (idebenone-treated and untreated). Measurement readings were taken at an absorbance of 405 nm at every 5 min for 30 min. The linear regression and standard curve were plotted.

Statistical analysis

Statistical analyses were performed on all the behavioral and biochemical assays. Means were used for the above studies including

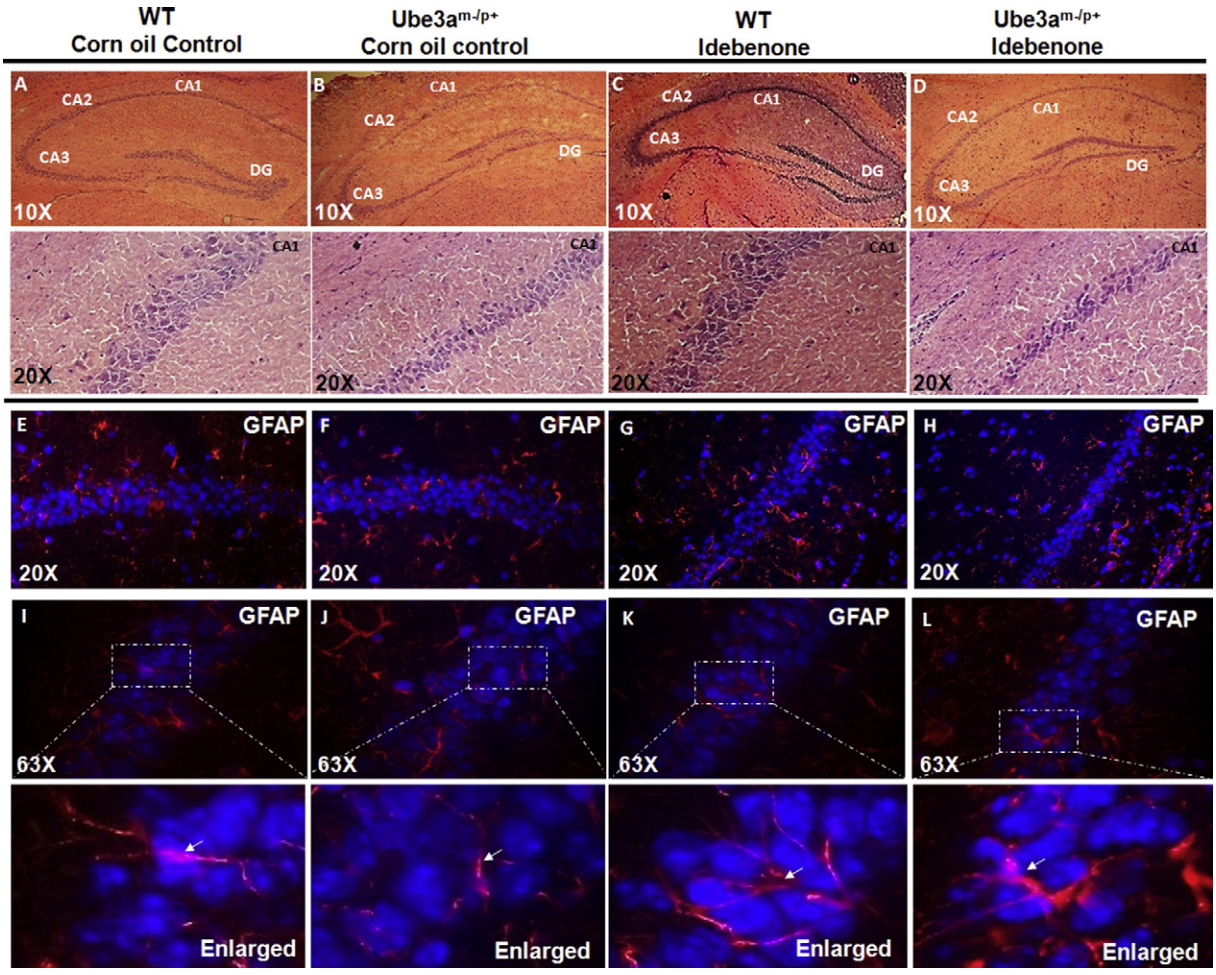

Fig. 2. Histological analysis of hippocampal regions and GFAP expression in WT and *Ube3a*$^{m-/p+}$ mice. A–D) H&E staining of corn oil control and idebenone-treated hippocampal CA1 (similar findings in CA2, CA3) and DG regions in the WT and *Ube3a*$^{m-/p+}$ mice. E–H) Immunohistochemical staining of GFAP expression levels in WT and *Ube3a*$^{m-/p+}$ mice treated with either corn oil or idebenone (200 mg/kg body weight) for 3 months. Each image was enlarged at a 63× magnification. Mice were analyzed per treatment group (n = 8–9). Arrows indicate positive GFAP staining of neuronal/glial cells.

weights, behaviors, enzyme activities, and protein expressions and statistically analyzed using mixed model analysis of variance (ANOVA). Statistical significance is denoted by $^{**}P \leq 0.001$ and $^{*}P \leq 0.005$.

Results

Idebenone treatment effects on motor coordination and behavioral studies

To assess the effects of idebenone administration on motor coordination we performed Rotarod testing. *Ube3a*$^{m-/p+}$ mice showed significantly reduced performance levels on the Rotarod, compared to the control wild type mice. Rotarod testing in the *Ube3a*$^{m-/p+}$ corn-oil treated mice demonstrated an increase in the latency to fall (in seconds) over a 3 month period, suggestive of a progressive cognitive impairment. However, after a 3-month idebenone regimen, *Ube3a*$^{m-/p+}$ mice showed significantly improved performance levels compared to their sex- and age-matched littermates, thereby suggesting improved motor coordination (Fig. 1A).

We next used a marble burying assay to evaluate neophobia (Yin et al., 2012), anxiety (Yin et al., 2012; Celio et al., 2006; Post, 2010;

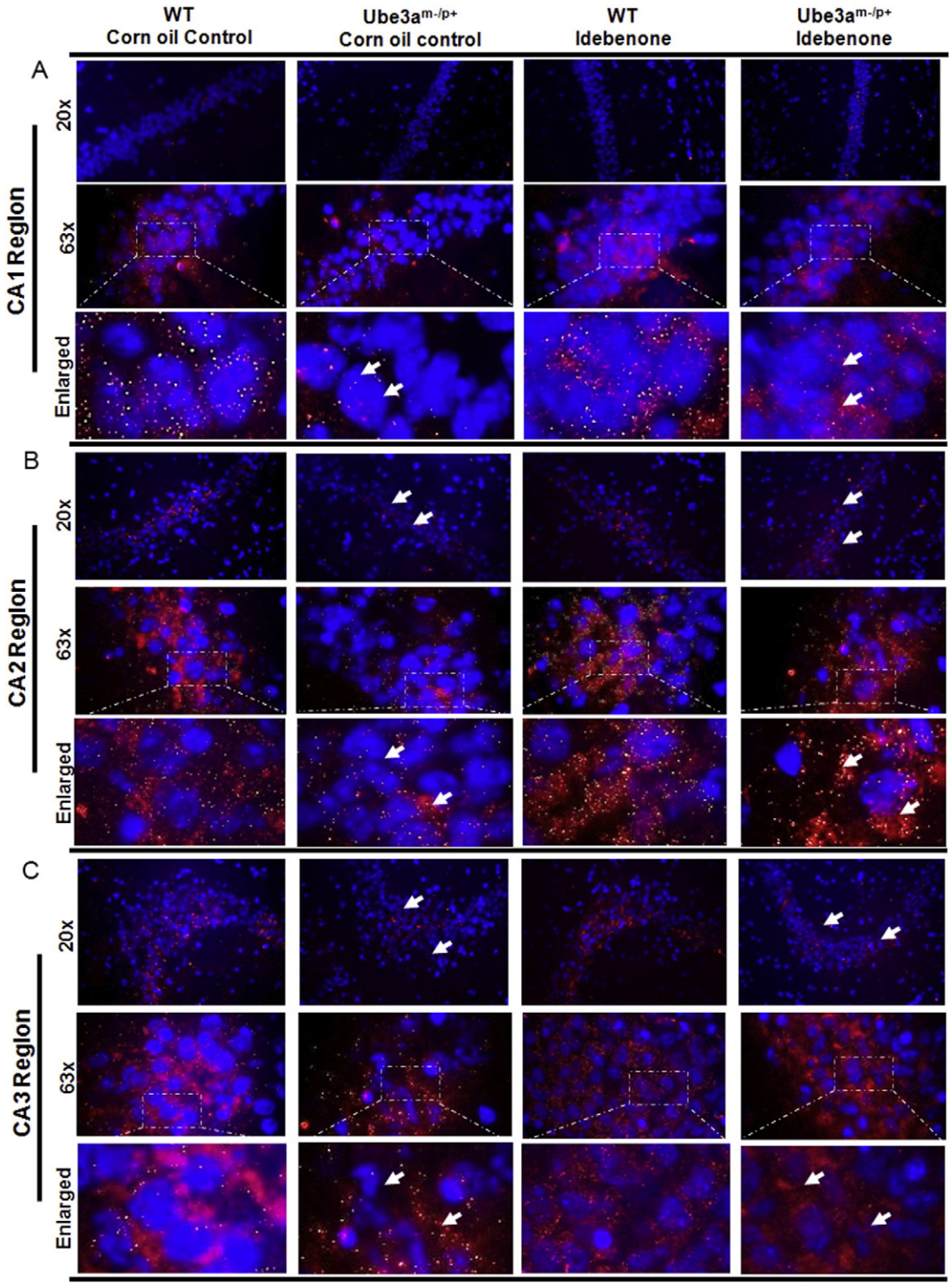

Fig. 3. Immunohistochemical analysis of complex III in hippocampal regions CA1, CA2, and CA3 in WT and *Ube3a*$^{m-/p+}$ mice. (A–C) Immunohistochemistry of complex III in hippocampal regions CA1, CA2, and CA3 in WT and *Ube3a*$^{m-/p+}$ mice treated with either corn oil or idebenone (200 mg/kg body weight) for 3 months. Arrows indicating decreased expression of complex III corrected by idebenone treatment in CA1–3 neurons. Mice analyzed per treatment group ($n = 8$–9).

Torrente et al., 2007; Krupnick et al., 2008) and obsessive compulsive behavior (Zhang et al., 2005; Camirand et al., 2004; Shishkin et al., 2001). We found that the *Ube3a*$^{m-/p+}$ mice buried a significantly lesser number of marbles than their wild type controls. However, upon idebenone treatment, the number of marbles buried by the *Ube3a*$^{m-/p+}$ mice increased significantly resembling the WT mice (Fig. 1B).

We chose the social index study based on prior literature (Huang et al., 2013). We found that *Ube3a*$^{m-/p+}$ mice did not have a reduced social index when compared to their wild type littermates and was unaffected by idebenone treatment (Fig. 1C). Finally, the *Ube3a*$^{m-/p+}$ mice showed a significantly reduced preference for novel object recognition (NOR) test for memory recognition when compared to their wild type littermates. Upon idebenone treatment, the novel object recognition of the *Ube3a*$^{m-/p+}$ mice remained unchanged (Fig. 1D). We found that *Ube3a*$^{m-/p+}$ mice have reduced brain weight, when compared to their wild type littermates, and this was not significantly altered after 3 months of idebenone treatment (Figs. 1E and F).

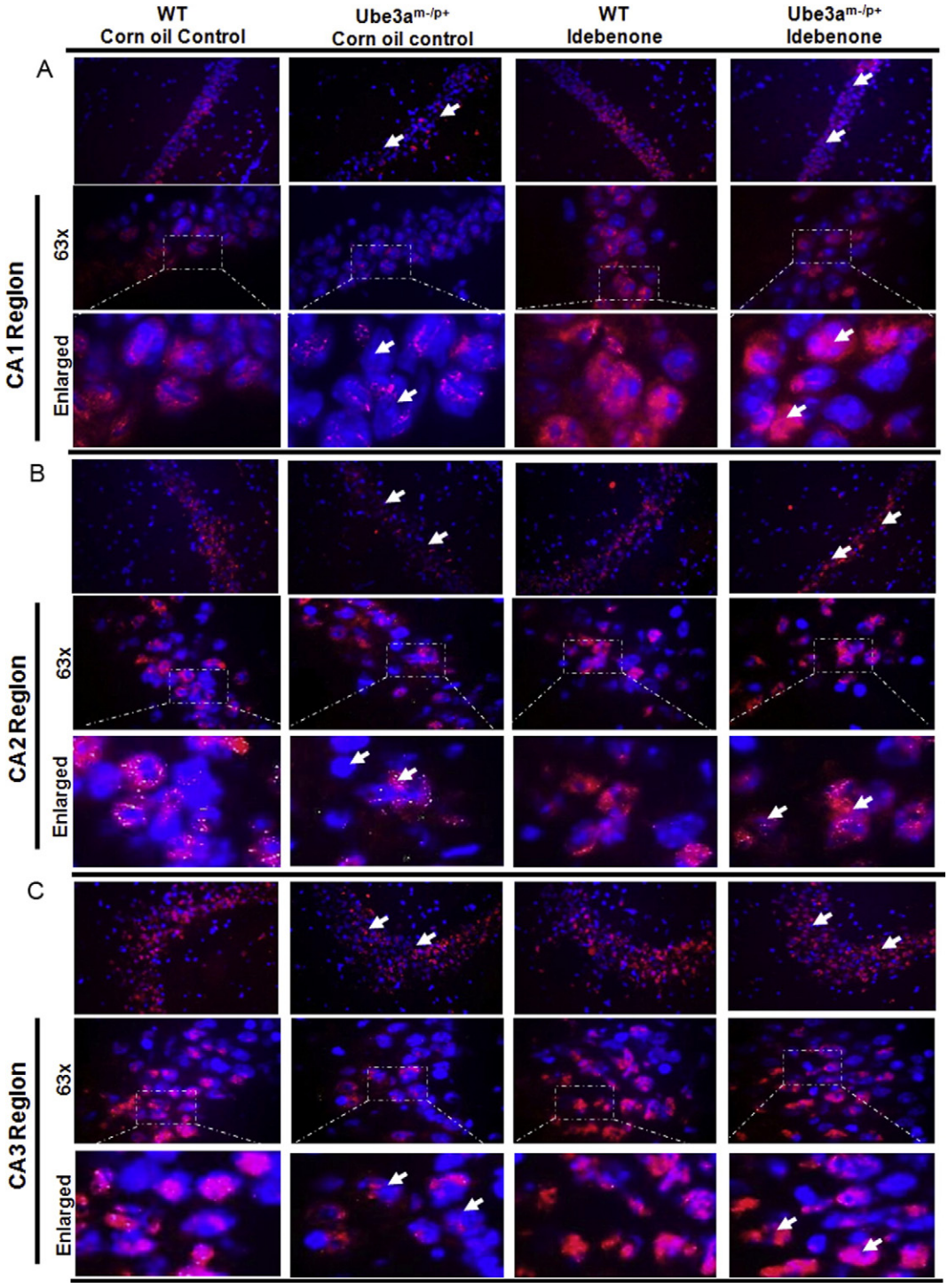

Fig. 4. Immunohistochemical analysis of complex IV in hippocampal regions CA1, CA2, and CA3 in WT and *Ube3a*$^{m-/p+}$ mice. (A–C) Immunohistochemistry of complex IV in CA1 hippocampal regions (also noted in CA2 and CA3) in WT and *Ube3a*$^{m-/p+}$ mice treated with either corn oil or idebenone (200 mg/kg body weight) for 3 months. Arrows indicating decreased expression of COX IV corrected by idebenone treatment in CA1, CA2 and CA3 neurons. Mice analyzed per treatment group (n = 8–9).

Histological analysis of hippocampal regions in the Ube3a$^{m-/p+}$ mice

First, we performed histological analyses to observe morphological differences in the hippocampal sections CA1, CA2, and CA3 regions in the treated and untreated WT and *Ube3a*$^{m-/p+}$ mice (Figs. 2A–D). No gross abnormalities were observed in the hippocampal architecture in treated and untreated WT and *Ube3a*$^{m-/p+}$ mice (Figs. 2A–D). We then confirmed the WT and *Ube3a*$^{m-/p+}$ hippocampal sections by staining with anti-GFAP to detect reactive astrocytes and found similar staining patterns in the hippocampal CA1, CA2, and CA3 regional sections, suggesting no pathological abnormalities in astrocyte expression (Figs. 2E–L).

Idebenone treatment improves expression of complexes III and IV in hippocampal CA1, CA2, and CA3 regions

In view of the previous studies, we investigated the effects of idebenone administration on complexes III and IV expression in *Ube3a*$^{m-/p+}$ mice by immunohistochemical and Western blot analyses. IHC of complex III showed reduced expression levels in the hippocampus CA1, CA2 and less pronounced in CA3 neurons (Figs. 3A–C). Interestingly, this deficiency was corrected in the CA1, CA2 and CA3 neurons after 3 months of idebenone treatment (Figs. 3A–C). A similar trend was observed with COX IV (cytochrome oxidase subunit IV) expression levels in the hippocampus CA1, CA2 and less pronounced in CA3 neurons of the *Ube3a*$^{m-/p+}$ mice when compared to the wild type littermates (Figs. 4A–C). Interestingly, this deficiency was also corrected in the CA1, CA2 and CA3 neurons after 3 months of idebenone treatment (Figs. 4A–C).

Idebenone treatment improves complexes III and IV in the hippocampus and cerebellum

Western blot analyses to quantify the complexes III and IV deficiencies from whole hippocampus mitochondria extract revealed decreased complexes III and IV expression in *Ube3a*$^{m-/p+}$ mice, which was corrected with idebenone treatment (Fig. 5A). Protein expression of complex III from whole cerebellum mitochondria was also reduced in *Ube3a*$^{m-/p+}$ mice, and partially corrected with idebenone treatment (Fig. 5B) compared to corn oil treated *Ube3a*$^{m-/p+}$ mice. In addition, complexes I, and II, and 4-hydroxynonenal (4-HNE) were analyzed, however no significant differences were detected between control and treated *Ube3a*$^{m-/p+}$ mice (Figs. 5A, 5B). Densitometric analyses on complexes I, II, III, and IV, and 4-HNE in control and treated *Ube3a*$^{m-/p+}$ mice were performed. Complexes III and IV from hippocampal mitochondrial samples from *Ube3a*$^{m-/p+}$ untreated mice showed significantly reduced expression levels (Fig. 5C). Complexes III from cerebellum mitochondrial samples from *Ube3a*$^{m-/p+}$ untreated mice showed significantly reduced expression levels (Fig. 5D).

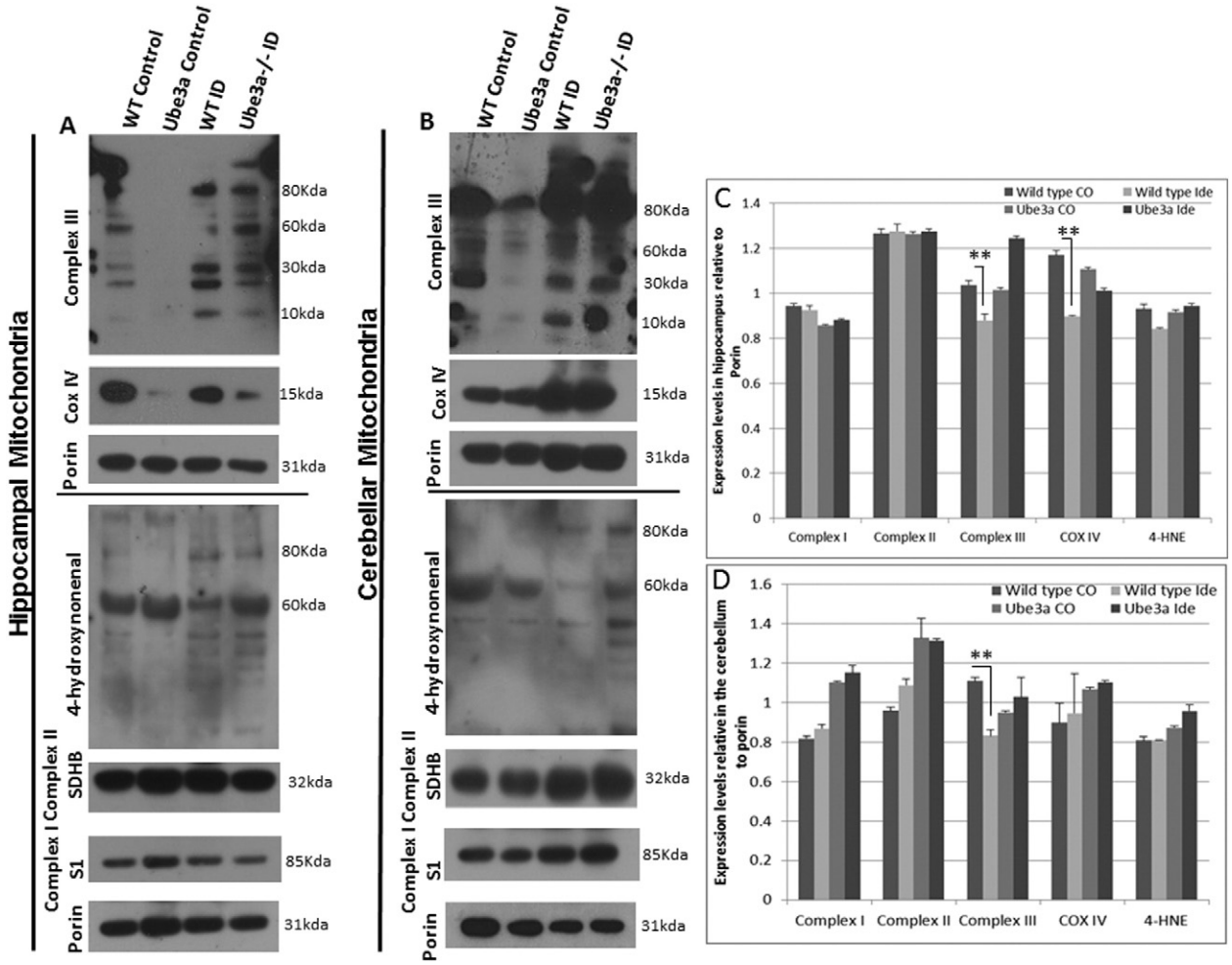

Fig. 5. Complexes I–IV protein expression in the hippocampus and cerebellar of WT and *Ube3a*$^{m-/p+}$ mice. Western blot of complexes I, II, III, and IV and 4-HNE expression from mitochondria extracted from the A) hippocampus or B) cerebellum, of WT and Ube3a$^{m-/p+}$ mice treated with either corn oil or idebenone (200 mg/kg body weight) for 3 months. Densitometric analyses in C) hippocampus and D) cerebellum. Mice analyzed per treatment group (n = 8–9). Statistical significance is denoted by **P ≤ 0.001.

Idebenone does not improve complexes III activity in the hippocampus and cerebellum

Activities of complexes I, II, and III from the control and treated *Ube3a*$^{m-/p+}$ mice were measured and analyzed. Activity levels of complexes I and II were unchanged in the *Ube3a*$^{m-/p+}$ mice hippocampus and cerebellum (Figs. 6A–D). However, complex III activity was found to be significantly reduced in the hippocampus mitochondria in *Ube3a*$^{m-/p+}$ mice, and was partially corrected after idebenone treatments, however, the difference was not significant (Fig. 6E). In contrast, complex III activity was partially reduced in the cerebellum from untreated *Ube3a*$^{m-/p+}$ mice, however, was not significant (Fig. 6F).

Seizure activity and electroencephalogram (EEG) testing

Seizure activity of WT and *Ube3a*$^{m-/p+}$ mice (idebenone-treated and untreated) was monitored. Seizures were induced by scratching forceps across the metal grating of the mouse cage lids. The stimulus did not depend on the lid being in physical contact with the cage, thus, the seizures were audiogenically-induced. Inducible seizures (lasting 10–20 s) were found in *Ube3a*$^{m-/p+}$ untreated mice (4/12), however, no seizures were detected upon idebenone administration (Supplemental Table 1). These seizures were epileptic-like including full body movements and stretching of limbs, monitored visually. Follow-up EEG testing was performed. No abnormal EEGs were detected in either WT or the treated *Ube3a*$^{m-/p+}$ mice (Supplemental Fig. 1A). However, the untreated *Ube3a*$^{m-/p+}$ demonstrated abnormal EEG (1/3 animals), which included high voltage 1.5-Hz slow wave with superimposed fast activity followed by 2–4 Hz rhythmic discharge (Supplemental Fig. 1B).

Idebenone treatment effects on oxidative stress levels in hippocampus and cerebellum

Because CoQ_{10} can have antioxidant properties, we assessed oxidative stress by determining the glutathione (GSH) activity and 4-hydroxynonenal (4-HNE) levels in *Ube3a*$^{m-/p+}$ mice. We measured total GSH levels in the hippocampus and cerebellum of treated and untreated WT and *Ube3a*$^{m-/p+}$ and found no significant differences (Table 1). The GSSG:GSH ratio was significantly increased in treated and untreated *Ube3a*$^{m-/p+}$ as compared to WT hippocampus ($P \leq 0.005$) and cerebellum ($P \leq 0.005$) samples, illustrating increased oxidative stress in the *Ube3a*$^{m-/p+}$ mice (Table 1). Interestingly, there was a slight decrease in the GSSG:GSH ratio levels in the hippocampus of the treated versus untreated *Ube3a*$^{m-/p+}$ animals ($P \leq 0.05$), however, this decrease was not observed in the cerebellum of these mice.

Discussion

Currently, investigations are underway to determine the underlying pathophysiological mechanism(s) in Angelman syndrome (AS) for the development of effective strategies/therapeutics, since there is currently no cure available. AS occurs with a frequency of approximately 1:15,000–1:25,000 live births and has been linked to deletions in the maternal chromosome region 15q11q13, paternal uniparental disomy, deficient imprinting center or *UBE3A* deletion or point mutations, as first shown by Ledbetter et al., 1981 (Ledbetter et al., 1981). It is now known that AS results from the loss of function of the *UBE3A* gene from the maternal chromosome only (Kishino et al., 1997; Knoll et al., 1989; Matsuura et al., 1997). Characterization of the classical symptoms include severe mental retardation, sleep disorders, seizures, limited speech, dysmorphic features and a characteristic electroencephalography (EEG) appearance with high voltage slow-wave activity. Affected individuals exhibit a happy demeanor, inappropriate laughter and excitability. With age, the clinical features of AS are altered whereby seizures decrease in frequency and EEG abnormalities are not observed. However, the facial features remain recognizable with age. Herein, we hypothesized that the CoQ_{10} analogue would restore the electron carrier flow pathway, thereby, improving the motor coordination, behavioral and mitochondrial dysfunction observed in *Ube3a*$^{m-/p+}$ Angelman mice.

Recently, there are several Angelman mouse models, having a deletion of the maternal UBE3A copy (Jiang et al., 1998a; Jiang et al., 1998b; Cattanach et al., 1997). These mice exhibit pathology characteristic of

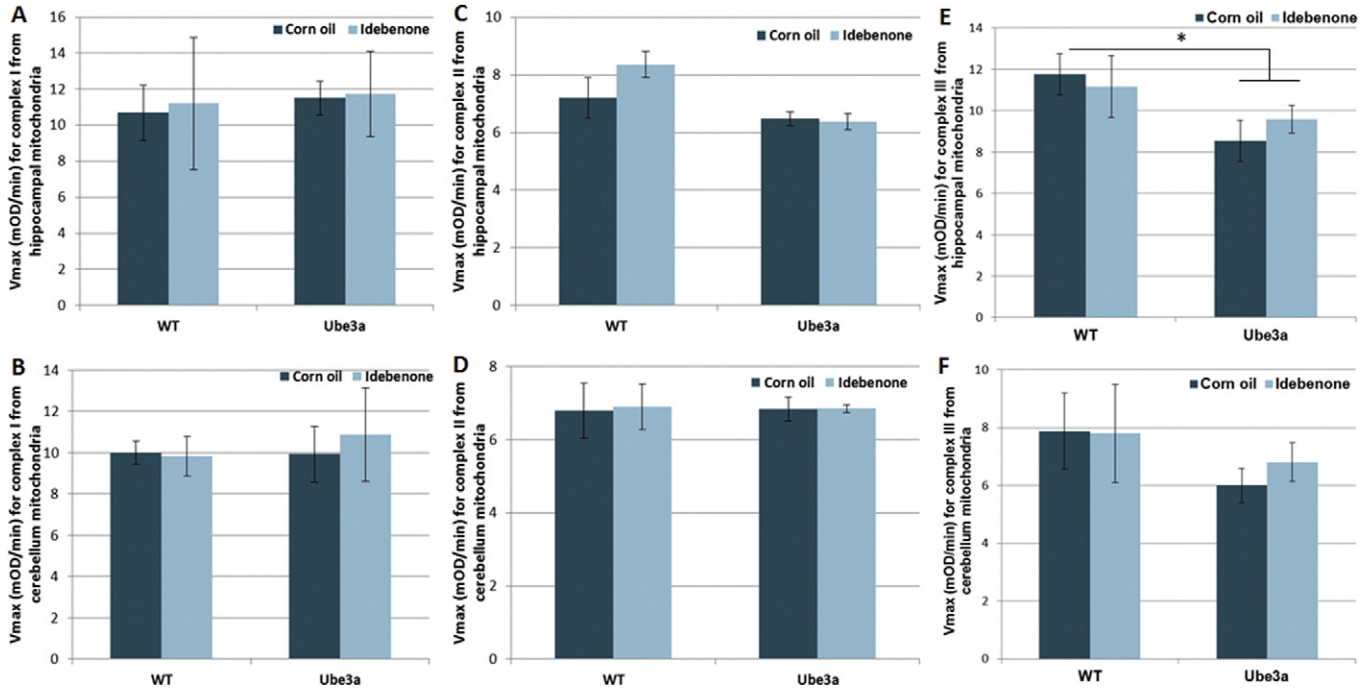

Fig. 6. Complexes I–III activities in the hippocampus and cerebellar of WT and *Ube3a*$^{m-/p+}$ mice. Vmax (mOD/min) from extracted mitochondria of WT and Ube3am−/p + mice treated with either corn oil or idebenone (200 mg/kg body weight) for 3 months of complex I in A) hippocampus and B) cerebellum, complex II in C) hippocampus and D) cerebellum, and complex III in E) hippocampus and F) cerebellum. Mice analyzed per treatment group (n = 8–9). Statistical significance is denoted by *P ≤ 0.005.

Table 1
GSH levels in *Ube3a*$^{m-/p+}$ mutant mice.

	Total GSH (nmol/mg) protein	Reduced GSH (nmol/mg) protein	GSSG (nmol/mg) protein	GSSG:GSH ratio
Cerebellum				
Wild type control	10.3 ± 0.027	9.6 ± 0.032	0.69 ± 0.04	7.28 ± 3.38
Wild type idebenone	15 ± 0.06	14.32 ± 0.074	0.71 ± 0.068	4.99 ± 1.69
Ube3a$^{m-/p+}$ control	10.86 ± 0.07	9.63 ± 0.033	1.22 ± 0.042**	12.73 ± 2.82**
Ube3a$^{m-/p+}$ idebenone	14.19 ± 0.034	12.73 ± 0.051	1.45 ± 0.051	11.41 ± 4.35
Hippocampus				
Wild type control	10 ± 0.08	8.88 ± 0.029	1.18 ± 0.036	13.34 ± 2.56
Wild type idebenone	10.57 ± 0.031	9.67 ± 0.054	0.89 ± 0.037	9.27 ± 2.83
Ube3a$^{m-/p+}$ control	9.93 ± 0.24	8.12 ± 0.068	1.8 ± 0.26**	22.26 ± 2.17**
Ube3a$^{m-/p+}$ idebenone	9.05 ± 0.031	7.68 ± 0.022	1.36 ± 0.017*	17.8 ± 1.51

Statistical significance is denoted by ** P = 0.005 and *P = 0.05.

Angelman syndrome, including motor coordination issues (ataxia), microcephaly, epileptic-like seizures and abnormal EEGs. These mice also display defects in the hippocampal long-term potentiation and cerebellar motor function (Huang et al., 2013; Gabriel et al., 1999). Cattanach et al. (1997) demonstrated abnormal EEG pathology, high voltage 1.5 Hz slow wave with superimposed fast activity followed by 2–4 Hz rhythmic discharge (Cattanach et al., 1997). Similarly, our untreated mouse model depicted the same abnormal EEG pathologies in the *Ube3a*$^{m-/p+}$ mice (Jiang et al., 1998b; Cattanach et al., 1997). However, this abnormal EEG pattern was not observed upon idebenone treatment in the *Ube3a*$^{m-/p+}$ mice, suggesting idebenone may improve seizure activity in AS patients.

One of the significant questions yet to be addressed has been the mechanism(s) at play in the pathophysiology underlying AS. Presumably, defective *UBE3A* activity results in failure to degrade its substrates because of impaired ubiquitination. *UBE3A* encodes the protein E6-AP and recently sacsin has been proposed as a substrate for E6-AP (Greer et al., 2010). Defects in *Sacsin* gene have been associated with a form of spastic ataxia (Gregianin et al., 2013). However, much remains to be understood regarding how deletion of *UBE3A* results in the observed AS neurodevelopmental deficits, including motor coordination and function. The study by Su et al. (2011) found a mitochondrial dysfunction in CA1 hippocampal neurons of *Ube3a*$^{m-/p+}$ Angelman mice (Su et al., 2011). In this report, the authors demonstrated abnormal mitochondria as well as a partial oxidative phosphorylation defect. The mechanism for this finding, however, is uncertain, though it could be related to the epigenetic methylation regulation of the respiratory chain protein expression. They suggested that *Ube3a* deficiency is associated with small mitochondria with abnormal cristae and dense spheroids and deficiency of complex III.

In this study, our findings indicate that idebenone administration resulted in the improvement of Rotarod performance test, marble burying assays, as well as increased expressions of complexes III and IV in the hippocampal and cerebellar neurons. These improvements may be related to increasing the energy production in the mitochondrial respiratory chain by increasing the electron flow from complexes I and II to complexes III and IV. Our preliminary seizure activity and EEG data suggests that idebenone may also improve seizure occurrence in AS patients. Future studies will focus on uncovering any amelioration of seizure activity in our *Ube3a*$^{m-/p+}$ mice with idebenone treatment.

Oxidative stress plays a role in synaptic and cognitive deficits in the mouse model of Angelman syndrome as well as many other neurodevelopmental disorders such as Rett syndrome, fragile X syndrome, tuberous sclerosis complex, autism, Alzheimer's disease, among others (De Felice et al., 2014; Hayashi et al., 2012; Kaur et al., 2014; Subash et al., 2014a; Subash et al., 2014b; Valenti et al., 2014). Based on our results, the potency of idebenone to improve mitochondrial electron flow and decrease the oxidative stress may be a consequence of its combined antioxidant function. Although idebenone administration reduced GSSH:GSH ratio levels, it was only significant in the hippocampus of *Ube3a*$^{m-/p+}$ Angelman mice. Levels of 4-HNE in *Ube3a*$^{m-/p+}$ Angelman mice were not significant. Therefore, it is likely that idebenone is having a direct effect on the bioenergetics rather than oxidative stress levels in this study. The recognition of these biochemical alterations may help in designing or developing therapeutic methods aimed at alleviating these symptoms.

Disorders of the mitochondrial respiratory chain (MRC) constitute a group of multisystemic diseases resulting from mutations in nuclear or mitochondrial DNA. Studies by Ernster and Dallner (1995) showed that CoQ_{10} is the predominant form of ubiquinone in humans, serves as an electron carrier in the MRC, and functions as a potent lipid soluble antioxidant (Ernster & Dallner, 1995). Treatment for MRC disorders has been difficult and to date the agents which have shown some therapeutic potential include CoQ_{10} and its synthetic analogues. The therapeutic potential of CoQ_{10} extends to not only disorders of CoQ_{10} biosynthesis, but also to other mitochondrial diseases including Leber's Hereditary Optic Neuropathy (LHON), Kearns–Sayre syndrome, mitochondrial DNA depletion syndrome and some neurological diseases (Heitz et al., 2012; Rodriguez et al., 2007). Herein, we report administration of idebenone, a CoQ_{10} analogue that improves motor coordination, mitochondrial respiratory chain complex expression and activity in the *Ube3a*$^{m-/p+}$ mouse model. This study suggests that improvement in respiratory chain function may have clinical therapeutic benefits in patients with Angelman syndrome.

Supplemental Fig. 1. EEG recordings of treated and untreated *Ube3a*$^{m-/p+}$ mice. A) Normal EEG before seizure induction in an untreated *Ube3a*$^{m-/p+}$ mouse. B) Abnormal EEG after seizure induction in an untreated *Ube3a*$^{m-/p+}$ mouse.

Funding sources

This research was supported by Cody's Quest Foundation, and Center for Autism Research and Translation (CART). Funding was also provided by the Minority Access to Research Careers (MARC) Program, NIH Grant GM-69337 Undergraduate Research and Mentoring in the Biological Sciences (URM) NSF Grant DBI-0731655 to AG.

Supplementary data to this article can be found online at http://dx.doi.org/10.1016/j.nbd.2015.01.005.

Acknowledgments

The *Ube3a*$^{m-/p+}$ mice were a kind gift from Dr. Arthur L. Beaudet, M.D., Ph.D. from Baylor College of Medicine and Dr. Yong-hui Jiang, MD., Ph.D. from Duke University, NC. We would like to thank Dr. Julie Lauterborn, Ph.D. for her expert assistance with brain histology. We would also like to thank the laboratory of Dr. Lbachir Benmohamed, Ph.D., Department of Ophthalmology, University of California, Irvine, for assistance with the enzyme activity assays. We would also like to thank Dr. Daniele Piomelli, Ph.D. for his assistance and guidance with the social approach test. For the EEG study, we would like to thank Anh Bui and Hannah Kim from the Department of Anatomy and Neurobiology, University of California-Irvine for their technical assistance.

References

Angoa-Perez, M., Kane, M.J., Briggs, D.I., Francescutti, D.M., Kuhn, D.M., 2013. Marble burying and nestlet shredding as tests of repetitive, compulsive-like behaviors in mice. J. Vis. Exp. 50978.

Badadani, M., Nalbandian, A., Watts, G.D., Vesa, J., Kitazawa, M., et al., 2010. VCP associated inclusion body myopathy and Paget disease of bone knock-in mouse model exhibits tissue pathology typical of human disease. PLoS ONE 5, e13183.

Bailus, B.J., Segal, D.J., 2014. The prospect of molecular therapy for Angelman syndrome and other monogenic neurologic disorders. BMC Neurosci. 15, 76.

Bird, L.M., 2014. Angelman syndrome: review of clinical and molecular aspects. Appl. Clin. Genet. 7, 93–104.

Camirand, G., Rousseau, J., Ducharme, M.E., Rothstein, D.M., Tremblay, J.P., 2004. Novel Duchenne muscular dystrophy treatment through myoblast transplantation tolerance with anti-CD45RB, anti-CD154 and mixed chimerism. Am. J. Transplant. 4, 1255–1265.

Cattanach, B.M., Barr, J.A., Evans, E.P., Burtenshaw, M., Beechey, C.V., et al., 1992. A candidate mouse model for Prader–Willi syndrome which shows an absence of SNRPN expression. Nat. Genet. 2, 270–274.

Cattanach, B.M., Barr, J.A., Beechey, C.V., Martin, J., Noebels, J., et al., 1997. A candidate model for Angelman syndrome in the mouse. Mamm. Genome 8, 472–478.

Celio, G.J., Padamsee, M., Dentinger, B.T., Bauer, R., McLaughlin, D.J., 2006. Assembling the fungal tree of life: constructing the structural and biochemical database. Mycologia 98, 850–859.

Condie, J., Goldstein, J., Wainwright, M.S., 2010. Acquired microcephaly, regression of milestones, mitochondrial dysfunction, and episodic rigidity in a 46, XY male with a de novo MECP2 gene mutation. J. Child Neurol. 25, 633–636.

De Felice, C., Signorini, C., Leoncini, S., Pecorelli, A., Durand, T., et al., 2014. Oxidative stress and Rett syndrome. Minerva Pediatr. 66, 41–62.

Ernster, L., Dallner, G., 1995. Biochemical, physiological and medical aspects of ubiquinone function. Biochim. Biophys. Acta 1271, 195–204.

Gabriel, J.M., Merchant, M., Ohta, T., Ji, Y., Caldwell, R.G., et al., 1999. A transgene insertion creating a heritable chromosome deletion mouse model of Prader–Willi and Angelman syndromes. Proc. Natl. Acad. Sci. U. S. A. 96, 9258–9263.

Gold, W.A., Williamson, S.L., Kaur, S., Hargreaves, I.P., Land, J.M., et al., 2014. Mitochondrial dysfunction in the skeletal muscle of a mouse model of Rett syndrome (RTT): implications for the disease phenotype. Mitochondrion 15, 10–17.

Greer, P.L., Hanayama, R., Bloodgood, B.L., Mardinly, A.R., Lipton, D.M., et al., 2010. The Angelman syndrome protein Ube3A regulates synapse development by ubiquitinating arc. Cell 140, 704–716.

Gregianin, E., Vazza, G., Scaramel, E., Boaretto, F., Vettori, A., et al., 2013. A novel SACS mutation results in non-ataxic spastic paraplegia and peripheral neuropathy. Eur. J. Neurol. 20, 1486–1491.

Hasegawa, S., Ichiyama, T., Sonaka, I., Ohsaki, A., Okada, S., et al., 2012. Cysteine, histidine and glycine exhibit anti-inflammatory effects in human coronary arterial endothelial cells. Clin. Exp. Immunol. 167, 269–274.

Hayashi, M., Miyata, R., Tanuma, N., 2012. Oxidative stress in developmental brain disorders. Adv. Exp. Med. Biol. 724, 278–290.

Heitz, F.D., Erb, M., Anklin, C., Robay, D., Pernet, V., et al., 2012. Idebenone protects against retinal damage and loss of vision in a mouse model of Leber's hereditary optic neuropathy. PLoS ONE 7, e45182.

Huang, H.S., Burns, A.J., Nonneman, R.J., Baker, L.K., Riddick, N.V., et al., 2013. Behavioral deficits in an Angelman syndrome model: effects of genetic background and age. Behav. Brain Res. 243, 79–90.

Jiang, Y., Tsai, T.F., Bressler, J., Beaudet, A.L., 1998a. Imprinting in Angelman and Prader–Willi syndromes. Curr. Opin. Genet. Dev. 8, 334–342.

Jiang, Y.H., Armstrong, D., Albrecht, U., Atkins, C.M., Noebels, J.L., et al., 1998b. Mutation of the Angelman ubiquitin ligase in mice causes increased cytoplasmic p53 and deficits of contextual learning and long-term potentiation. Neuron 21, 799–811.

Kaidanovich-Beilin, O., Lipina, T., Vukobradovic, I., Roder, J., Woodgett, J.R., 2011. Assessment of social interaction behaviors. J. Vis. Exp. 48, e2473. http://dx.doi.org/10.3791/2473.

Kaur, K., Chauhan, V., Gu, F., Chauhan, A., 2014. Bisphenol A induces oxidative stress and mitochondrial dysfunction in lymphoblasts from children with autism and unaffected siblings. Free Radic. Biol. Med. 76C, 25–33.

Kishino, T., Lalande, M., Wagstaff, J., 1997. UBE3A/E6-AP mutations cause Angelman syndrome. Nat. Genet. 15, 70–73.

Knoll, J.H., Nicholls, R.D., Magenis, R.E., Graham Jr., J.M., Lalande, M., et al., 1989. Angelman and Prader–Willi syndromes share a common chromosome 15 deletion but differ in parental origin of the deletion. Am. J. Med. Genet. 32, 285–290.

Krupnick, A.S., Gelman, A.E., Okazaki, M., Lai, J., Das, N., et al., 2008. The feasibility of diaphragmatic transplantation as potential therapy for treatment of respiratory failure associated with Duchenne muscular dystrophy: acute canine model. J. Thorac. Cardiovasc. Surg. 135, 1398–1399.

Ledbetter, D.H., Riccardi, V.M., Airhart, S.D., Strobel, R.J., Keenan, B.S., et al., 1981. Deletions of chromosome 15 as a cause of the Prader–Willi syndrome. N. Engl. J. Med. 304, 325–329.

Matsuura, T., Sutcliffe, J.S., Fang, P., Galjaard, R.J., Jiang, Y.H., et al., 1997. De novo truncating mutations in E6-AP ubiquitin-protein ligase gene (UBE3A) in Angelman syndrome. Nat. Genet. 15, 74–77.

Nalbandian, A., Llewellyn, K.J., Kitazawa, M., Yin, H.Z., Badadani, M., et al., 2012. The homozygote VCP(R155H/R155H) mouse model exhibits accelerated human VCP-associated disease pathology. PLoS ONE 7, e46308.

Nalbandian, A., Llewellyn, K.J., Badadani, M., Yin, H.Z., Nguyen, C., et al., 2013. A progressive translational mouse model of human valosin-containing protein disease: the VCP (R155H/+) mouse. Muscle Nerve. 47, 260–270.

Nicholls, R.D., Saitoh, S., Horsthemke, B., 1998. Imprinting in Prader–Willi and Angelman syndromes. Trends Genet. 14, 194–200.

Post, S.G., 2010. In defense of myoblast transplantation research in preteens with Duchenne muscular dystrophy. Pediatr. Transplant. 14, 809–812.

Rodriguez, M.C., MacDonald, J.R., Mahoney, D.J., Parise, G., Beal, M.F., et al., 2007. Beneficial effects of creatine, CoQ10, and lipoic acid in mitochondrial disorders. Muscle Nerve 35, 235–242.

Shishkin, S.S., Terekhov, S.M., Krokhina, T.B., Shakhovskaia, N.I., Podobedova, A.N., et al., 2001. Dystrophin gene expression in patients with Duchenne muscular dystrophy after myoblast transplantation. Genetika 37, 1104–1111.

Silverman, J.L., Yang, M., Lord, C., Crawley, J.N., 2010. Behavioural phenotyping assays for mouse models of autism. Nat. Rev. Neurosci. 11, 490–502.

Silvers, J.M., Harrod, S.B., Mactutus, C.F., Booze, R.M., 2007. Automation of the novel object recognition task for use in adolescent rats. J. Neurosci. Methods 166, 99–103.

Su, H., Fan, W., Coskun, P.E., Vesa, J., Gold, J.A., et al., 2011. Mitochondrial dysfunction in CA1 hippocampal neurons of the UBE3A deficient mouse model for Angelman syndrome. Neurosci. Lett. 487, 129–133.

Subash, S., Essa, M.M., Al-Asmi, A., Al-Adawi, S., Vaishnav, R., et al., 2014a. Pomegranate from Oman alleviates the brain oxidative damage in transgenic mouse model of Alzheimer's disease. J. Tradit. Complement. Med. 4, 232–238.

Subash, S., Essa, M.M., Al-Asmi, A., Al-Adawi, S., Vaishnav, R., et al., 2014b. Effect of dietary supplementation of dates in Alzheimer's disease APPsw/2576 transgenic mice on oxidative stress and antioxidant status. Nutr. Neurosci. http://dx.doi.org/10.1179/1476830514Y.0000000134.

Torrente, Y., Belicchi, M., Marchesi, C., D'Antona, G., Cogiamanian, F., et al., 2007. Autologous transplantation of muscle-derived CD133+ stem cells in Duchenne muscle patients. Cell Transplant. 16, 563–577.

Valenti, D., de Bari, L., De Filippis, B., Henrion-Caude, A., Vacca, R.A., 2014. Mitochondrial dysfunction as a central actor in intellectual disability-related diseases: an overview of Down syndrome, autism, Fragile X and Rett syndrome. Neurosci. Biobehav. Rev. 46, 202–217.

Yin, H.Z., Nalbandian, A., Hsu, C.I., Li, S., Llewellyn, K.J., et al., 2012. Slow development of ALS-like spinal cord pathology in mutant valosin-containing protein gene knock-in mice. Cell Death Dis. 3, e374.

Zhang, C., Chen, W., Xiao, L.L., Tan, E.X., Luo, S.K., et al., 2005. Allogeneic umbilical cord blood stem cell transplantation in Duchenne muscular dystrophy. Zhonghua Yi Xue Za Zhi 85, 522–525.

Update

Neurobiology of Disease
Volume 78, Issue , June 2015, Page 56

DOI: https://doi.org/10.1016/j.nbd.2015.03.024

Neurobiology of Disease 78 (2015) 56

Contents lists available at ScienceDirect

Neurobiology of Disease

journal homepage: www.elsevier.com/locate/ynbdi

Corrigendum

Corrigendum to "Administration of CoQ10 analogue ameliorates dysfunction of the mitochondrial respiratory chain in a mouse model of Angelman Syndrome" [Neurobiol. Dis. 76C (2015) 77–86]

Katrina J. Llewellyn[a,*], Angèle Nalbandian[a,d], Arianna Gomez[a], Don Wei[b], Naomi Walker[a], Anh Bui[c,d], Hannah Kim[c,d], Ivan Soltesz[c,d], Virginia E. Kimonis[a,d,**]

[a] Department of Pediatrics, Division of Genetics and Genomics, 2501 Hewitt Hall, University of California-Irvine, Irvine, CA 92697, USA
[b] Department of Anatomy & Neurobiology, Gillespie Hall, University of California-Irvine, Irvine, CA 92697, USA
[c] Department of Anatomy & Neurobiology, University of California-Irvine, Irvine, CA 92697, USA
[d] Center for Autism Research and Treatment, University of California-Irvine, Irvine, CA 92697, USA

The authors regret the omission of three authors from the originally published article. The correct author listing is reflected above. In addition, Fig. 5 contained an error in the published article. The corrected figure appears below.
The authors would like to apologise for any inconvenience caused.

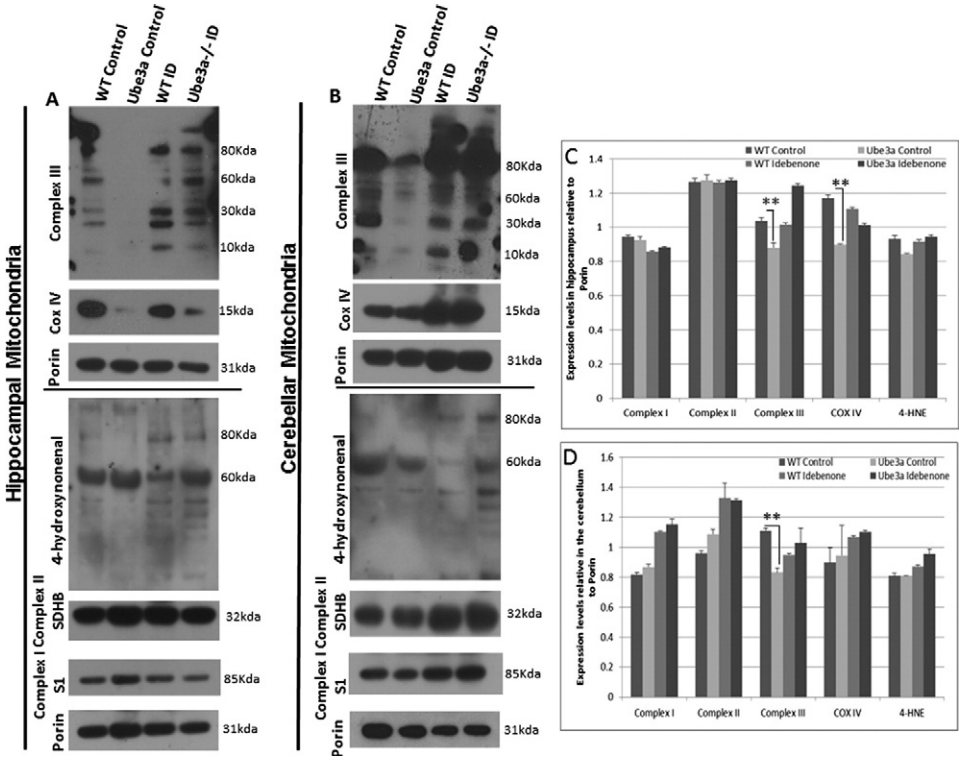

DOI of original article: http://dx.doi.org/10.1016/j.nbd.2015.01.005.
* Corresponding author.
** Correspondence to: V.E. Kimonis, Department of Pediatrics, Division of Genetics and Genomics, 2501 Hewitt Hall, University of California-Irvine, Irvine, CA 92697, USA.
E-mail addresses: kllewell@uci.edu (K.J. Llewellyn), vkimonis@uci.edu (V.E. Kimonis).

http://dx.doi.org/10.1016/j.nbd.2015.03.024